Journal of Applied Polymer Science

Study of molecular weight and chain branching architectures of natural rubber

Wei Qu, Yong Zhu, Guangsu Huang, Cheng Huang, Ming-Chao Luo, Jing Zheng
State Key Laboratory of Polymer Material Engineering, College of Polymer Science and Engineering, Sichuan University, Chengdu 610065, People's Republic of China
Correspondence to: G. Huang (E-mail: guangsu-huang@hotmail.com)

ABSTRACT: The origin of the unique bimodal molecular weight distribution (MWD) of natural rubber (NR) has been controversial up to now. Studying the connection between particle size and molecular weight (MW) might be a key approach to revealing the mystery of NR architectures. In this study, through constructing NR models as objectives and employing gel-permeation chromatography coupled to a viscosity detector as well as a multiangle laser light scattering detector (GPC-DP-MALLS), we have acquired branching parameters for NR from solid experiments and data fitting. It is found that small rubber particles (SRPs) and large rubber particles (LRPs) jointly construct the unique bimodal MWD of NR. SRPs with low branching numbers (Bn) and branching frequency (λ) are believed to be composed of almost linear rubber molecules having no chain-end groups to be branched. In contrast, LRPs transform their MWD curve into a clear bimodal peak after transesterification and possess high Bn. Meanwhile, the formation of branch points in LRP by hydrogen bonding and ionic linkages has been clearly confirmed. Thus, a clear and exact structure of NR has been revealed for the first time. © 2016 Wiley Periodicals, Inc. J. Appl. Polym. Sci. **2016**, *133*, 43975.

KEYWORDS: phospholipids; properties and characterization; proteins; rubber

Received 16 January 2016; accepted 24 May 2016
DOI: 10.1002/app.43975

INTRODUCTION

Natural rubber (NR) from *Hevea brasiliensis* is a very important commercial source of elastomers. Solid NR consists of approximately 94% rubber hydrocarbon and 6% nonrubber components such as lipids, proteins, and fatty acids. It has been recognized for a long time that the proteins and lipids from natural rubber latex play an important role in stabilizing the latex particles and endowing NR with outstanding properties.[1]

NR has been presumed to contain two kinds of different functional groups at both initiating and terminating ends, referred to as ω and α terminals, respectively. The ω-terminal is a dimethylallyl group linked to protein by hydrogen bonding, whereas α-terminal has been postulated to link with monophosphate or diphosphate groups associated with phospholipids.[2,3] It is found that the molecular weight of NR from different clones of *Hevea* trees has either a distinctly bimodal distribution with high- and low-molecular-weight (MW) peaks or a unimodal distribution with a shoulder in the low-MW region.[4] Two mainstream opinions are suggested to interpret this phenomenon. The first mainstream opinion ascribes the bimodal character to the chain branching in NR, where the high MW fraction is composed of the lower one through branch points derived from both terminals.[5] As a proof, deproteinization of NR using a proteolytic enzyme with a surfactant can decompose the branch points at the ω-terminal in NR.[6,7] Transesterification of deproteinized NR (DPNR) in a toluene solution with sodium methoxide decomposes the residual branch points at the α-terminal to give NR with a bimodal molecular weight distribution (MWD).[6] However, the addition of small amounts of polar solvents in the toluene decreases the gel content in DPNR drastically.[1,3,8] This phenomenon indicates that branch points mainly come from the association of phospholipids via hydrogen bonding, whereas the existence of branch points in DPNR originates from ionic linkages between negative charges of phospholipids with divalent cations, and the latter case is considered to be an inferior effect.[3,9–11] The other opinion points out that the synthesis of NR molecules is catalyzed by rubber transferases, and there are two types of rubber transferase in NR that respectively exist on the surface of small rubber particles (SRP) and large rubber particles (LRP). SRPs from fresh *Hevea* latex are supposed to have higher rubber transferase activity than LRP, and both of their activities are governed by the age of the rubber trees. Because of the different enzyme catalytic activities, NR produces high- and low-MW rubber molecules that correspond to a bimodal MWD.[12,13] But so far neither has provided enough evidence because of the complexity of the natural network

structure. Nevertheless, the bimodal MWD pattern of NR is retained even after the decomposition of all the branch points by deproteinization and transesterification, which suggests that the MWD characteristics of NR are not only due to branching, but are also involved in the mechanism of rubber biosynthesis.[14,15] One piece of evidence is that the MW of NR increases with increasing age of the *Hevea* tree. Furthermore, the relative intensity of the peak of the high-MW fraction rises with increased age of the tree, though the peak positions ascribed to low- and high-MW fractions are independent of the tree age.[14]

It is widely accepted that NR is synthesized within latex particles, and there are two different particle sizes that exist in rubber serum and cream. The chain-propagation process catalyzed by enzymatically active proteins is performed by the successive addition of isopentenyl diphosphate to the diphosphate terminal group. The rubber particles in the serum fraction, having an active diphosphate group, are presumed to form almost linear molecules with high-MW fraction, whereas the rubber particles in the cream fraction are thought to be composed of rubber molecules containing long-chain fatty acid esters, terminated with the terminal group with which the molecules are terminated.[16,17] REF and SRPP, two *Hevea brasiliensis* proteins, are believed to be the rubber elongation factors in NR biosynthesis. SRPP may have the higher elongation efficiency.[18,19] REF has amyloid properties and could quickly form large aggregates (>μm). Thus, rubber particles are believed to be involved in different growth mechanisms that control the molecular weight of NR.[16–20]

Then the connection between particle size and molecular weight becomes a key issue in revealing NR architectures. Although numerous research studies on molecular weight and branched chains of NR have been reported,[21–25] none of them offers direct and clear evidence. Also, the previously mentioned works are mostly based on conjectures instead of experimental data, because the absolute MW of NR cannot be detected by gel-permeation chromatography (GPC), due to its poor solubility. Fortunately, as a development of contemporaneous measurement techniques, gel-permeation chromatography coupled with a viscosity detector and a multiangle laser light scattering detector (GPC-DP-MALLS) can allow a direct determination of absolute M_w, radius of gyration (Rg), hydrodynamic radius (Rh), and viscosity (η). Through a combination of M_w and size parameters (Rh or Rg), in the case of polydisperse polymers, one can obtain information about the shape of the polymer chains and the distribution of branched chains depending on the size or molar mass.[26,27] As a consequence, a branching characterization by this advanced approach will promise an exact understanding of NR architecture.

An attempt was made in this study to clarify the relationship between the particle size and MW of NR. Regarding the clear changes in MW and MWD after esterification compared to the small changes after deproteinization, we adopted DPNR as a model to study. First of all, fractionation of DPNR-latex by centrifugation with different speed rates was carried out to obtain the fractions of different particle sizes. All the fractions of DPNR were subjected to transesterification to decompose the branch points. The combination of the results from the molecular weight analysis by GPC and the branching characterization of the DPNR fractions clearly illustrates the relationship between particle size and MW of NR. Secondly, in order to ascertain the role of hydrogen bonding and ionic linkage in the formation of branch points, further experiments were carried out to decompose the branch points by treating DPNR with polar solvents and diammonium hydrogen phosphate (DAHP). GPC analysis and branching characterization by GPC-DP-MALLS were applied for this purpose.

EXPERIMENTAL

Materials and Sample Preparation

Commercial High ammonia (HA) NR latex from the *H. brasiliensis* tree was provided by China Hainan Industry Group, Hainan, China. The NR latex was adjusted to dry rubber content (DRC) at 30% w/v and subjected to deproteinization by incubation with 0.04% w/v protease (P 5380, Sigma, United states) in the presence of 0.5% w/v Triton X-100 [Kelong, Chengdu, China analytical reagent (AR) grade] at 37 °C for 8–16 h. The resulting latex was centrifuged at 12,000 rpm for 40 min. The rubber cream fraction was redispersed in 1% of ammonium hydroxide (Kelong) and adjusted to a 30% DRC. The process was repeated twice. The last cream fraction was tiled on a polyester film and dried at 30 °C *in vacuo*. Free fatty acids or nonlinked fatty acids were removed by acetone extraction in a Soxhlet apparatus for 48 h.

Transesterification of the rubber from acetone-extracted DPNR (AE-DPNR) was carried out in 1.5% w/v toluene by reacting with freshly prepared sodium methoxide and stirring at 40 °C for 6 h. The resulting TE-DPNR was obtained by the precipitation of the rubber solution with an excess of methanol (AR grade) and then was tiled on the polyester film and dried at 30 °C *in vacuo*, removing free fatty acids or nonlinked fatty acids as mentioned above.

The treatment of DPNR latex with DAHP was performed by the addition of 5% w/v DAHP into DPNR-latex (20% DRC), followed by incubation with stirring for 24 h at room temperature (25 °C). Then the cream fraction was obtained through centrifugation at 12,000 rpm for 40 min, which was followed by redispersing in 0.1% Triton X-100 and recentrifuging at 12,000 rpm for 40 min. Dried rubber was obtained by coagulating the latex with an excess of methanol and drying *in vacuo* at 30 °C.

The polar solvent treatment was taken by using various solvents such as methanol, ethanol, and acetic acid (LabScan, England, AR grade). It was carried out by the addition of 1–3% v/v polar solvent to a toluene solution at a concentration of 1% w/v AE-DPNR, followed by stirring at room temperature for 24 h. The resulting solid rubber was obtained by pouring the rubber solution into an excess amount of methanol (AR grade) and drying *in vacuo* at 30 °C, followed by acetone extraction in a Soxhlet apparatus to remove free fatty acids or nonlinked fatty acids, as mentioned above.

The fractionation of fresh deproteinized latex was carried out by centrifugation at different speed rates to separate the rubber into

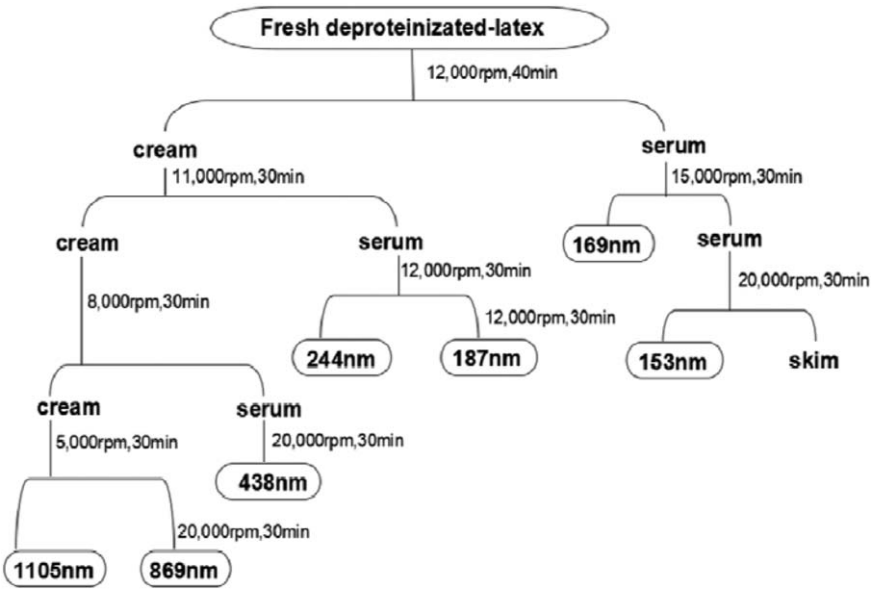

Figure 1. The fractionation steps of fresh deproteinized latex by particle sizes.

seven fractions of different particle sizes successively, according to the previous paper.[21] The fractionation step of DPNR is shown in Figure 1. First, 12,000 rpm for 40 min was applied to separate the cream and serum. The resulting rubber cream fraction was redispersed into 0.1% v/v Triton X-100 to make 20% DRC and then recentrifuged five times with different speed rates to get the the other fractions. To avoid coagulation of the rubber particles, the centrifugation procedure was done under 5 °C. Each fraction was collected by casting rubber cream onto the polyester film and drying at 30 °C *in vacuo*, followed by acetone extraction for 24 h in a Soxhlet extractor to remove the free fatty acids and their esters. The solid fractionated rubber was prepared at 1.5% w/v in a toluene solution and further subjected to transesterification with freshly prepared sodium methoxide ($NaOCH_3$) at 40 °C for 6 h. TE-DPNR was purified by precipitation of the rubber solution into an excess of methanol and then was tiled on the polyester film and dried at 30 °C *in vacuo*, removing free fatty acids or nonlinked fatty acids, as mentioned above.

Characterization

Determination of Molecular Weight. The MW and MWD of the NR samples were determined by gel-permeation chromatography (HLC-8320GPC, TOSOH, Japan) with two columns in series, packed with crosslinked polystyrene gel and equipped with a differential refractive index detector. Tetrahydrofuran (THF, LabScan, HPLC grade) was used as an eluent with a flow rate of 0.6 mL/min at 40 ± 0.1 °C. The rubber samples were dissolved in THF (LabScan, HPLC grade) at a concentration of 0.05% w/v in THF and filtered through a prefilter and 0.45-μm membrane filter. Polyisoprene (PI) of narrow MWD was used as a standard.

Branching Characterization. The chain branching of rubber samples was charaterized by gel-permeation chromatography coupled with a viscosity detector and a multiangle light scattering detector (GPCmax VE-2001, Malvern, United states). Tetrahydrofuran was used as an eluent with a flow rate of 1 mL/min

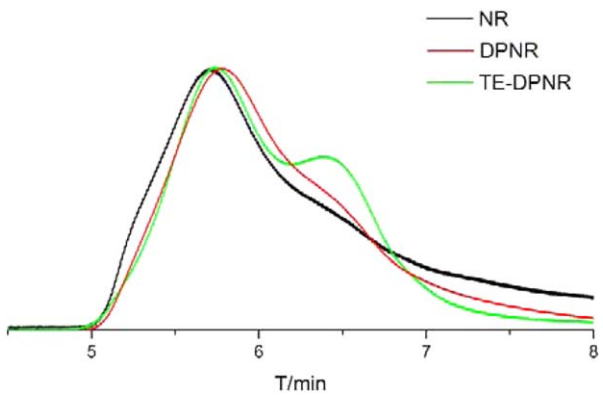

Figure 2. The molecular weight distributions of NR, DPNR, and TE-DPNR. [Color figure can be viewed in the online issue, which is available at wileyonlinelibrary.com.]

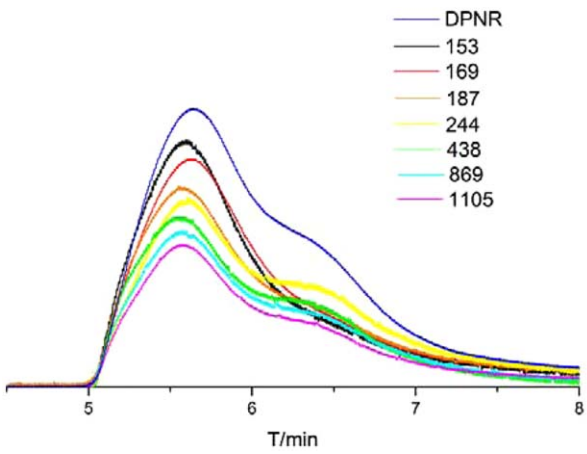

Figure 3. Molecular weight distribution of fractionated DPNR. [Color figure can be viewed in the online issue, which is available at wileyonlinelibrary.com.]

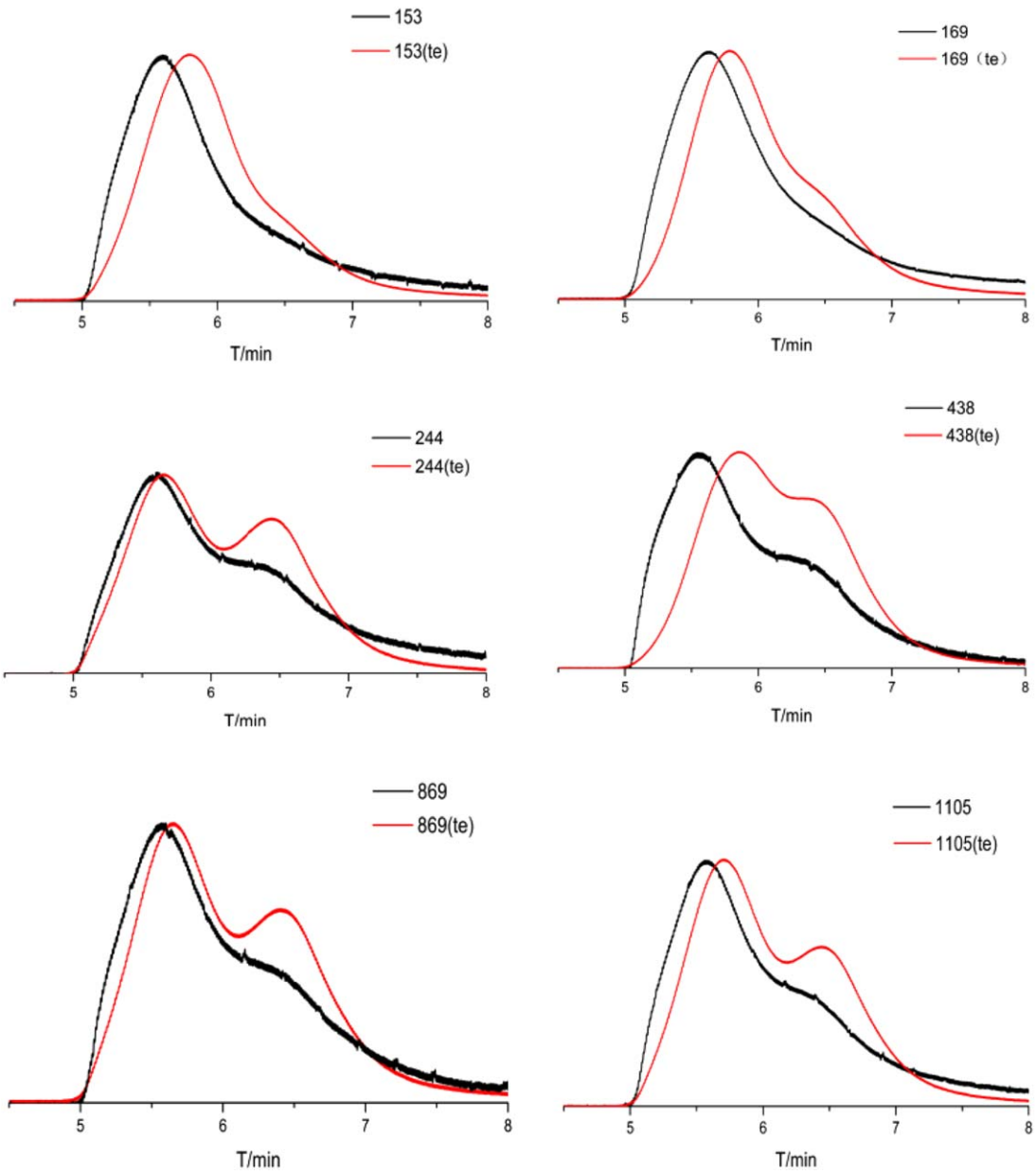

Figure 4. Molecular weight distribution of each fraction before and after transesterification. [Color figure can be viewed in the online issue, which is available at wileyonlinelibrary.com.]

at 40 ± 0.1 °C. High-cis PI was used as a standard linear homologue.

RESULTS AND DISCUSSION

NR Architectures and Molecular Weight Distribution

The distribution of NR molecular weight has been a controversial problem. To clarify this problem, we prepared three models, including NR, DPNR, and transesterified–deproteinized NR (TE-DPNR). N and P elemental analyses were performed in order to ascertain the effective removal of protein in DPNR and phospholipid in TE-DPNR, respectively. The deproteinization of NR decreases the N content from 0.5% to 0.1%, suggesting a little protein remains in DPNR. The P content is detected to be 65 ppm in TE-DPNR, which confirms the almost complete removal of phospholipids by transesterification. The MWDs of NR, DPNR, and TE-DPNR detected by GPC are shown in Figure 2. NR shows a unimodal MWD with a shoulder peak, while DPNR exhibits a similar pattern with a little shift to the low-MW region. Interestingly, the MWD curve of AE-DPNR transforms into an apparent bimodal peak after the esterification, and the low-MW fraction at the shoulder peak rises significantly, which is attributed to the formation of linear molecules. The results strongly support the assumption that phospholipid molecules construct the branch points in DPNR. Nevertheless, the fact that a high-MW fraction still notably exists instead of disappearing completely

Table 1. Branching Characterization Results for Fractionated Rubber Samples Detected by GPC-DP-MALLS Using Linear Standard PI as Reference

Sample	M_w (10^6)	M_w/M_n	Rh (nm)	Rg (nm)	α	log *K*	Branches per mole	Branch frequency
PI	0.993	1.656	44.390	68.932	0.683	−3.269	0	0
153	2.408	2.163	39.915	64.536	0.546	−3.155	98.599	0.054
169	1.483	1.795	42.804	72.193	0.556	−3.209	106.558	0.044
244	6.686	3.084	52.324	75.484	0.144	−0.804	424.379	0.074
438	5.521	3.292	37.986	67.836	0.642	−4.342	1180.462	0.639
1105	3.905	1.576	41.054	68.935	0.536	−3.421	455.671	0.136

seems to suggest that NR is composed of both linear macromolecular chains and long branched molecular chains as well, which has not been put forward yet.

An interesting problem is that if linear macromolecular chains and long branched chains coexist in NR, what approach they will adopt? To solve this puzzle, DPNR was fractionated by centrifugation under different speeds to obtain fractions of different particle sizes. The MWD curves of all fractions of different particle sizes are shown in Figure 3. It is evident that the SRPs having a mean diameter less than 250 nm exhibit a clear unimodal MWD. However, the LRPs with a mean diameter larger than 250 nm display a bimodal MWD with a small shoulder in the low-MW region.

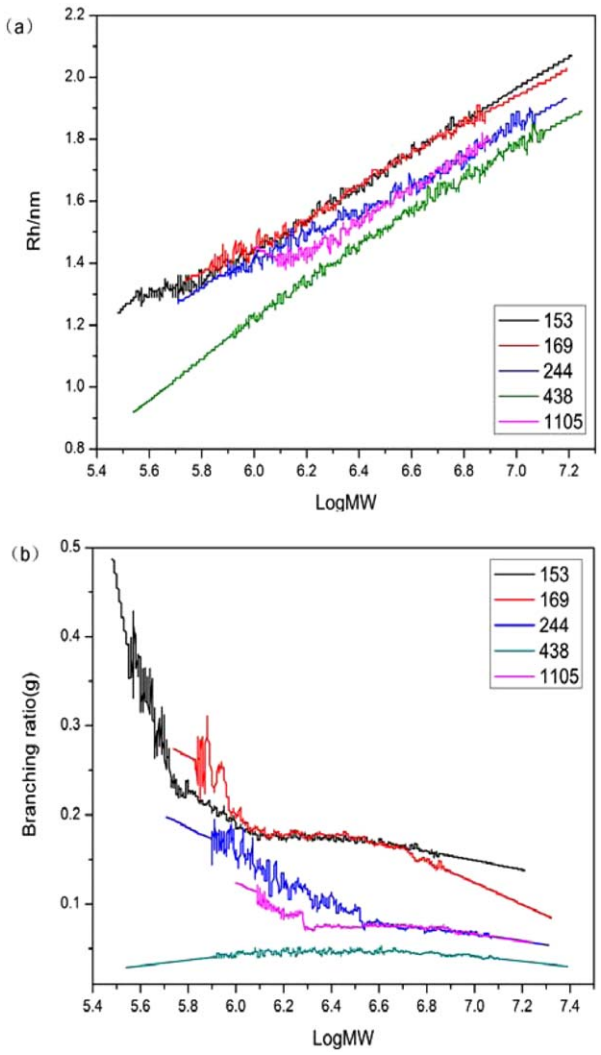

Figure 5. Distributions of (a) hydrodynamic radius, Rh, and (b) branching ratio, *g*, for fractionated DPNR samples as a function of molar mass using linear standard PI as reference. [Color figure can be viewed in the online issue, which is available at wileyonlinelibrary.com.]

Transesterification of each fraction was performed for further study. The MWD curves of each fraction before and after the treatment are shown in Figure 4. It is found that after transesterification the SRP still shows a clear unimodal MWD pattern, with just a little shift to the low-molecular-weight region, which indicates that there are no branch points derived from phospholipids existing in SRP. In contrast with the SRP, the LRP after transesterification is observed to produce an apparent bimodal MWD where the low-MW fraction at the original shoulder peak position rises significantly. These results strongly indicate that the MWD and particle sizes of NR do have a close relationship. In more detail, NR is composed of two kinds of molecules, linear macromolecules in SRP and branched molecules in LRP, which are involved in different growth mechanisms of MW.

Particle Dimensions with NR Branching Parameters

One usually can only measure the soluble fraction by GPC, due to the natural crosslinked structure of NR, and therefore make a rough comparison of MW. Fortunately, the absolute MW of branched rubber can be perfectly determined by GPC-DP-MALLS through the fitting of branching in NR. In terms of a principle that branched polymer molecules have lower hydrodynamic volume, higher density, and lower intrinsic viscosity,[26,27] their molecular dimension is different from that of their linear molecular counterpart at the same MW, so by employing the GPC-DP-MALLS technique and comparing the relative sizes of branched and linear molecules in solution, the branching content can be determined.

Zimm and Stockmayer[27–29] take the intrinsic viscosity [η] to determine the branching ratio (*g*), with the relationship between [η] and hydrodynamic radius (Rh) shown in eq. (1):

$$g'_M = \frac{[\eta]_{M,Br}}{[\eta]_{M,Lin}} = \frac{Rh^3_{M,Br}}{Rh^3_{M,Lin}};\quad g'_M = g^{\varepsilon}_M s; \tag{1}$$

where Rh is the hydrodynamic radius of the samples, and ε is the structure factor. The subscripts Br and Lin represent the branched and linear chains, respectively.

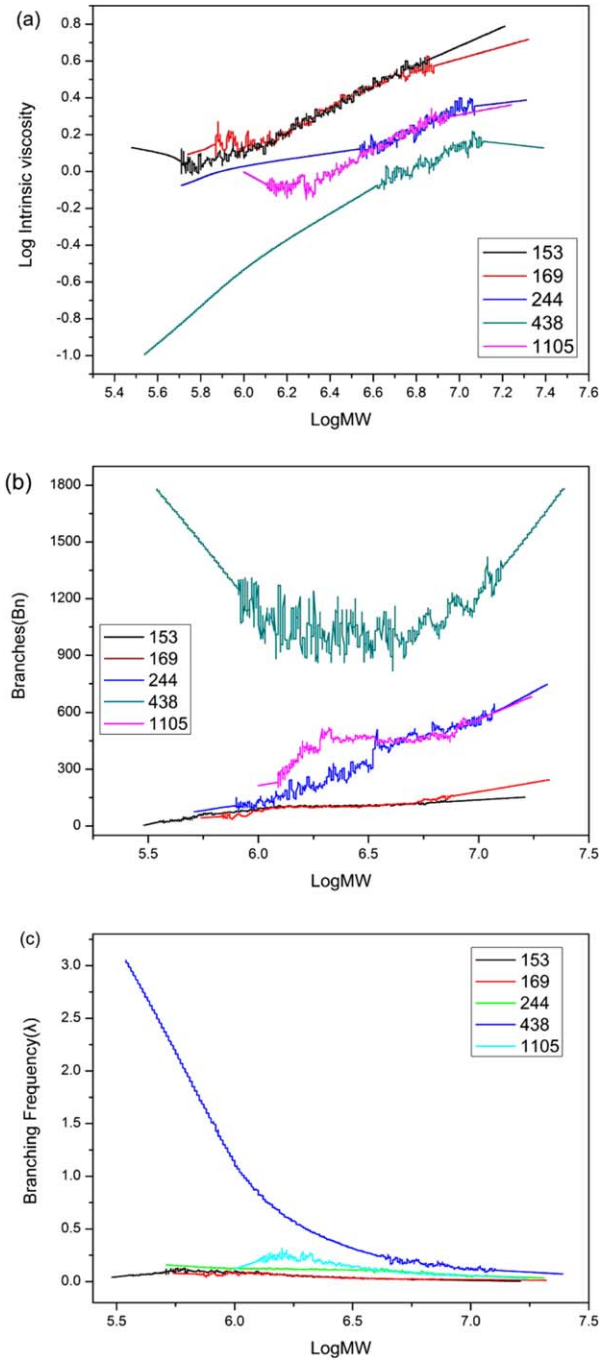

Figure 6. (a) Mark–Houwink plot, (b) distributions of the branching numbers, Bn, and (c) distributions of branching frequency for fractionated DPNR samples using linear standard PI as reference. [Color figure can be viewed in the online issue, which is available at wileyonlinelibrary.com.]

By adopting a random, trifunctional model (polydisperse), the number of branches per mole, B_M, can be calculated from the parameter g using the relation shown in eq. (2)[29]:

$$g=\frac{6}{B_M}\left[\frac{1}{2}\left(\frac{2+B_M}{B_M}\right)^{1/2}\ln\left(\frac{(2+B_M)^{1/2}+B_{M^{1/2}}}{(2+B_M)^{1/2}-B_{M^{1/2}}}\right)-1\right] \quad (2)$$

According to the phenomenon that branching number (Bn) will increase with the growth in molecular weight, the branch frequency is introduced to better characterize the branched structure:

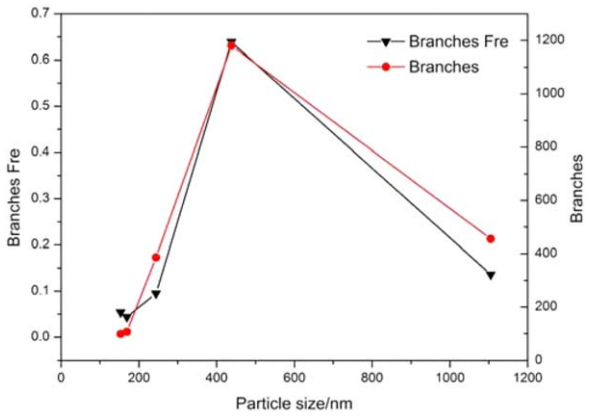

Figure 7. Distributions of branches and branching frequency of fractionated DPNR as a function of particle size. [Color figure can be viewed in the online issue, which is available at wileyonlinelibrary.com.]

$$\lambda(M_{w_i})=\frac{f(\text{repeat})\times \text{Bn}_i}{M_{w_i}} \quad (3)$$

where Bn_i is the branching number of each component of the molecular weight, M_{w_i} is the MW of each component, and f(repeat) is the repeat units.

From our conversant Mark–Houwink curve of log[η] against log M_w, a qualitative analysis of branching structure can be obtained, using the coefficient α and K of linear PI as standard. As the curve sinks, the degree of branching increases:

$$[\eta]=KM^{\alpha} \quad (4)$$

$$\log[\eta]=\log KM+\alpha M \quad (5)$$

In order to clarify the relationship between the particle size and molecular weight of NR, the rubber samples of 153, 169, 244, 438, and 1105 nm were selected as the representative sizes of fractionation for the branching characterization. For

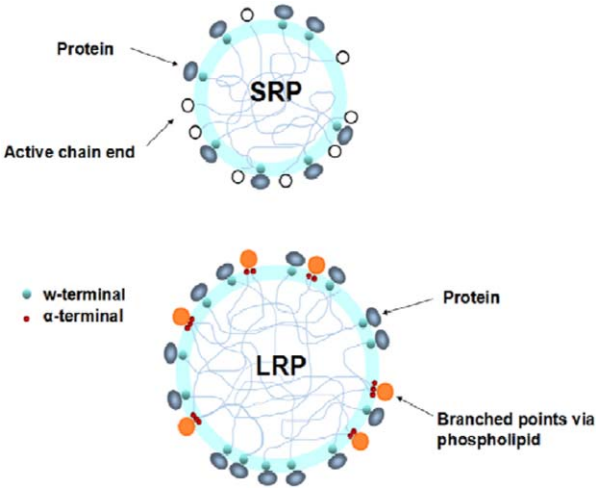

Figure 8. Presumed structure of small and large rubber particles in fresh latex. [Color figure can be viewed in the online issue, which is available at wileyonlinelibrary.com.]

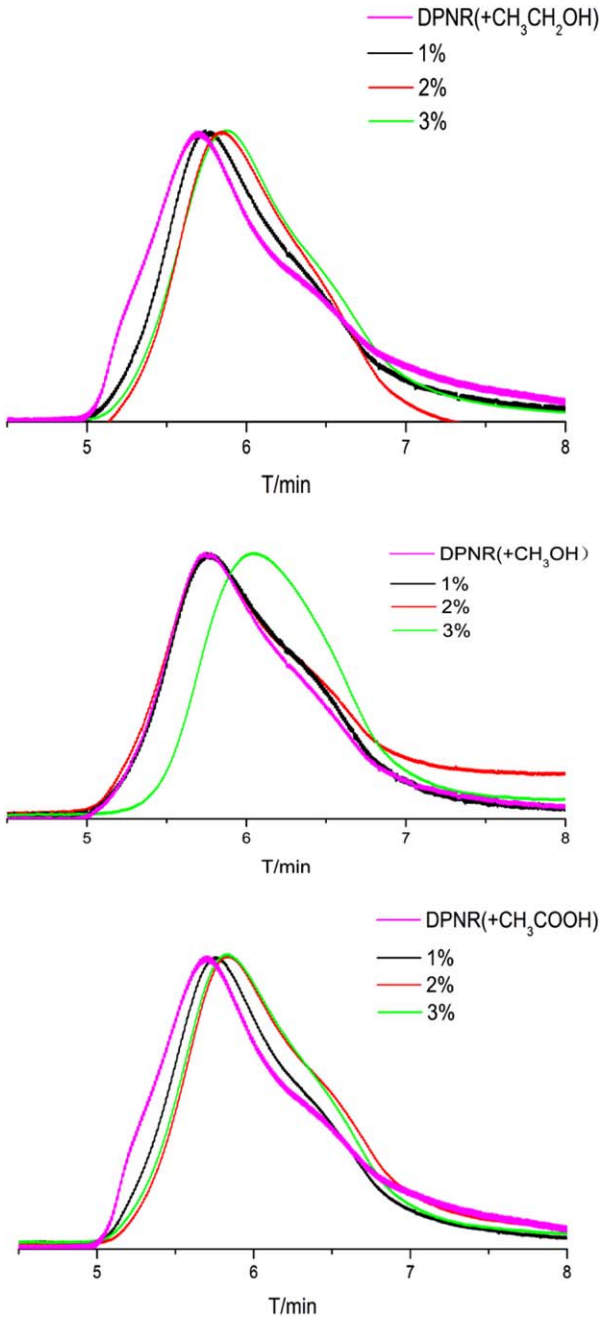

Figure 9. Molecular weight distribution of DPNR with treatment of polar solvent. [Color figure can be viewed in the online issue, which is available at wileyonlinelibrary.com.]

convenience, in further descriptions, we abbreviate the sample names as 153, 169, 244, 438, and 1105 nm, respectively, and PI as the model of zero branches is used as the linear standard. The branching parameters calculated from the above three equations are exhibited in Table 1. M_n refers to the number average molecular weight and M_w refers to the weight average molecular weight. Obviously, the sample of 438 nm has the highest branching number of 1180.4 per mol. The samples 153 and 169 nm only have a small Bn. The specific analysis of branching is stated as follows.

For a given molar mass, branched samples have a smaller hydrodynamic volume than their linear counterpart. The distributions of Rh, representing the conformation of rubber samples, are the most direct results to reflect the molecular architectures. As shown in Figure 5(a), the Rh values of the fractionated samples are observed to increase in line with the molar mass. For branched molecules at the same molar mass, Rh decreases as the branched density increases, resulting in a gentler slope for the curve of Rh versus log *M*. The curves of 153 and 169 nm almost overlap each other, showing the highest Rh, in contrast to that of 438 nm. In the case of the same MW, the rubbers with lower size should have higher degree of branching. Thus, we can have the preliminary deduction that the sample of 438 nm has the highest degree of branching than the other fractionated rubber samples, while the 153 and 169 nm samples display the lowest branching. Simultaneously, the branching ratio calculated from eq. (1) is shown in Figure 5(b). According to the equation, if g is less than 1, their molecule chains will be branched, such that the sample of 438 nm with the lowest g value has the highest branching degree compared to the other fractions in the whole range of MW, with little change as the MW increases. The values of the other sizes show a significant decrease as MW increases, which indicates that their molecules have more branching at higher molar mass.

To enable a visual comparison of branching between samples, taking a qualitative point of view, the Mark–Houwink plot was used by performing the calculation in eq. (5). Figure 6(a) shows the Mark–Houwink plot of fractionated DPNR samples as a function of molar mass. From the analysis above, the different values of [η] at the same MW could be used to compare the branching degree, the higher value indicating the lower branching. In addition, the more branched molecules display Mark–Houwink plots with gentler slopes compared to the linear one, which is used to provide an intuitive description of branching. As can be seen, the sample of 153 nm has the highest [η], similar to 169 nm; that is, it has a lower branching degree than the other samples. The 438 nm sample shows the gentlest plot with the lowest [η], indicating the highest degree of branching.

More branching parameters such as branching number (Bn) and branching frequency (λ) can be calculated by eq. (2) and eq. (3), where the λ we obtain in this experiment represents the branching number of 1000 MW units. The distributions of Bn and λ are plotted against molar mass, as shown in Figure 6(b,c), respectively. Apparently, the sample of 438 nm is observed to have the most branches in the whole range of MW, up to 1200 approximately. Its λ is also the highest and decreases greatly as the MW rises, which strongly demonstrates that 438 nm has the highest degree of branching. In contrast, there are few branches in the samples 153 and 169 nm, reaching the maximum values of 150 and 200, respectively, when the log MW increases to about 7.25, with λ close to zero. Meanwhile, 244 and 1105 nm show an intermediate value of Bn, and the highest values are also achieved when the log MW reaches the maximum at 7.25. The specific values of Bn and λ in average MW are plotted against particle sizes to give the branching distribution shown in Figure 7, from which the branching degree from high to low can be clearly seen to be 438, 1105, 244, 169,

Table 2. Molecular Weight Characteristics and Gel Content of AE-DPNR after Treatment with Polar Solvent by Incubation for 24 h at Room Temperature

Sample		M_n	M_w	M_w/M_n	Gel content (% w/w)
AE-DPNR		302,011	920,229	3.047	18.5
AE-DPNR + CH_3OH(v/v)	1%	286,090	880,773	3.079	15.1
	2%	199,659	896,282	4.489	12.7
	3%	212,145	484,678	2.285	6.8
AE-DPNR + CH_3CH_2OH(v/v)	1%	265,927	935,633	3.518	17.2
	2%	291,991	837,024	2.867	16.9
	3%	158,844	751,998	4.734	8.0
AE-DPNR + CH_3COOH(v/v)	1%	260,680	954,059	3.660	13.3
	2%	269,850	827,676	3.067	11.3
	3%	216,038	770,943	3.569	9.4

and 153 nm in turn. SRPs like 153 nm and 169 nm are observed to have almost no branches, while 244 nm has a little more branching than those with a λ of 0.074. In contrast, LRPs are found to be seriously branched, especially for 438 nm.

All of the above branching analysis confirms the speculation that SRPs are mostly linear molecules with almost no branches and may contain the active chain end for chain elongation. As expected, the LRPs have the branched points to form branched molecules. The difference in particle sizes that is caused by the biosynthesis mechanism controls the MWD. In other words, the coexistence of LRPs and SRPs makes NR construct its unique macromolecular architectures. This is an exact illustration based on solid branching parameters for the first time. The ω-terminal is a dimethylallyl group linked to protein, and α-terminal has been postulated to link with the monophosphate or diphosphate groups associated with phospholipids.[2,3] Futhermore, the NR particles are believed to have a core–shell structure made up of a hydrophobic core of molecules surrounded by a mixed layer of proteins and phospholipids.[5,30–32] Here, according to the structure of the rubber chain and NR particles above and by combination with the confirmatory structures of SRPs and LRPs, we can propose the specific architecture of NR latex particles shown in Figure 8. When NR particles merge, SRPs and LRPs will lose their interface and form a different network, which will be stated in further discussions below.

Architecture of Branch Points

How the branch points formed is a deep question concerning NR architectures. To focus on this, we performed a series of dissolution tests by adding the polar solvents methanol, ethanol, and acetic acid with concentrations of 1%, 2%, and 3% (w/v) into the rubber toluene solution. As shown in Figure 9, the MWDs of samples that have undergone the treatment of polar solvents all show a similar trend: they shift the high-MW peak toward the low-MW region, in comparison with DPNR. The larger addition, the more apparent shift is observed, which is quite consistent with the decrease in MW. We attribute the changes in MW and MWD to the destruction of hydrogen bonds that formed branch points at terminal groups. The gel content of AE-DPNR after treatment with the polar solvents is shown in Table 2. It is remarkable that after the addition of methanol, ethanol, and acetic acid with a concentration of 3% (v/v) to the rubber solution, the gel content of AE-DPNR drastically goes down from 16.5% to 6.8%, 8.0%, and 7.4%, respectively. This also signifies that the branch points in the network constructed by hydrogen bonding are decomposed effectively.

Nevertheless, the gel content remains at a certain level after the treatment with polar solvent, which implies that the branch points in DPNR originate partly from the aggregation of phospholipids and phosphate groups by hydrogen bonding, and there must exist some other connecting patterns at the terminal groups of rubber chains. Moreover, in comparison with transesterification of AE-DPNR, the treatment of AE-DPNR with polar solvents fails to change the MWD to a bimodal pattern, and the MW of AE-DPNR treated with polar solvents is much higher

Table 3. Gel Content of NR, DPNR, AE-DPNR, and TE-DPNR

Sample	NR	DPNR	AE-DPNR	TE-DPNR
Gel content (% w/w)	58.8	19.1	18.5	0

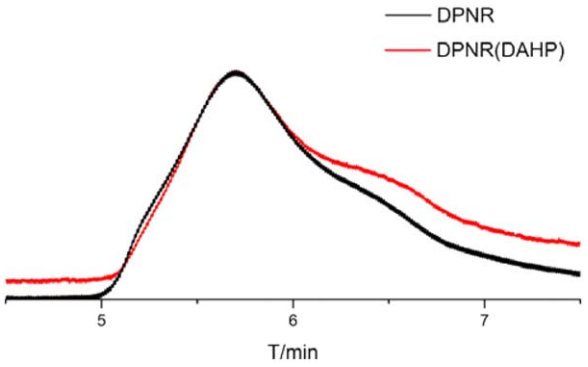

Figure 10. Molecular weight distribution of DPNR with treatment of DAHP. [Color figure can be viewed in the online issue, which is available at wileyonlinelibrary.com.]

Table 4. Molecular Weight Characteristics and Gel Content of DPNR after Treatment with 5% w/v DAHP into DPNR-latex (20% DRC)

Sample	M_n	M_w	M_w/M_n	Gel content (% w/w)
DPNR	283,466	1,031,905	5.108	18.5
DPNR + 5% DAHP	252,001	1,129,022	4.480	14.7

than TE-DPNR. These findings indicate that the AE-DPNR samples treated with polar solvents should have contained some branched molecules, while TE-DPNR is almost linear molecules without any gel content, as shown in Table 3, which is in good agreement with the viewpoint that the branch points in NR form not only by hydrogen bonding but are also derived from some other linkages, such as ion linkages or micelle formation.

The Mg^{2+} ion in latex, as a cofactor for rubber biosynthesis, has been reported to act to form branch points by ionic linkages between phosphate groups during storage of HA-latex.[11] DAHP is usually added to fresh latex to remove Mg^{2+} ions by centrifugation.[10,11] In the present work, the effect of Mg^{2+} ions on the branching formation was investigated by the addition of 5% (v/v) DAHP into DPNR-latex. The resultant MWD of DPNR-latex treated with DAHP as shown in Figure 10 illustrates that the addition of DAHP into DPNR latex causes a slight increase of MW in the low-MW region at the shoulder peak. However, no shift in MWD is detected, which signifies that the ionic crosslinks formed by Mg^{2+} have less effect on branching formation than the aggregation of phospholipid polar head groups via hydrogen bonding. Moreover, some results from Table 4 show that the gel content of DPNR after the treatment with DAHP slightly decreases from 18.5% to 14.7%, which also is regarded as powerful evidence for less effect of the Mg^{2+} ions.

The branching characterization of DPNR, TE-DPNR, 2% CH_3OH–treated AE-DPNR, and DAHP-treated DPNR was carried out to offer further evidence, with the results shown in Table 5. DPNR has an average Bn of 763.5 per mol, which is much higher than the 22.7 of TE-DPNR, strongly certifying the significant effect of phospholipids on branching formation. The Bn of 2% CH_3OH–treated DPNR is 437.3 per mol, about half the value of DPNR. However, DPNR exhibits only a slight decrease of Bn after the treatment with DAHP. Moreover, Bn is utilized for the fitting calculation of absolute MW instead of the MW of the soluble fraction detected by GPC, from which a real network structure will be revealed. Compared to DPNR with the highest MW, TE-DPNR with almost no branches shows a much lower MW, which demonstrates that the branched molecule of high MW is formed by linear chains through branching.

The distributions of Rh and g for the samples as a function of molar mass are shown in Figure 11(a,b). TE-DPNR has the highest Rh, no doubt due to its most linear chain, exhibiting good coincidence with the highest g value. Meanwhile, the Rh distribution plot of DPNR treated with DAHP almost overlaps that of DPNR, showing a similar g plot as well. Unexpectedly, AE-DPNR treated with 2% CH_3OH shows a lower Rh value than that of DPNR, which indicates the former has more branching for the same MW. This finding contradicts our previous speculation that the addition of polar solvent could destroy branch points formed by hydrogen bonding. Simultaneously, AE-DPNR treated with 2% CH_3OH presents the lowest g value with almost no change as MW increases, while DPNR and DPNR treated with 5% DAHP both show a little decrease at the low molar mass region.

Mark–Houwink plots of the samples (see Figure 12) exhibit similar results, where the sample of AE-DPNR treated with 2% CH_3OH has a lower [η] and is thought to have more branched chains than DPNR.

For a direct comparison of branching degree between samples, distributions of Bn and λ are plotted against MW, as shown in Figure 13(a,b), respectively. TE-DPNR with almost no Bn and λ in the whole range of MW is strongly confirmed to be linear molecules. The Bn distribution of DPNR treated with DAHP displays a tendency similar to that of DPNR, whose branches increase linearly with the molar mass. This illustrates that there are no significant changes of branching in DPNR after the treatment with DAHP, just having a small decrease of average Bn from 763.5 to 730.2 (Table 5).

It should be noted that the sample of AE-DPNR treated with 2% CH_3OH displays about half the Bn value of that of DPNR. Meanwhile, the distribution of Rh and g and even the Mark–Houwink plot all suggest that AE-DPNR treated with 2% CH_3OH has more chain branching than DPNR. This discrepancy could be explained reasonably by the assumption of the

Table 5. Branching Characterization Results of DPNR, TE-DPNR, 2% CH_3OH–treated-AE-DPNR, and DAHP-treated-DPNR Detected by GPC-DP-MALLS Using Linear Standard PI as Reference

Sample	M_w (10^6)	M_w/M_n	Rh (nm)	Rg (nm)	α	log K	Branches per mole	Branch frequency
PI	0.993	1.656	44.390	68.932	0.683	−3.269	0	0
DPNR	5.352	2.172	42.015	60.710	0.515	−3.411	763.579	0.202
TE-DPNR	0.770	1.739	27.540	43.007	0.679	−3.671	22.799	0.033
2% CH_3OH	4.169	2.880	32.301	41.725	0.585	−4.024	437.318	0.222
DAHP	4.850	2.525	39.702	62.937	0.463	−3.097	730.259	0.203

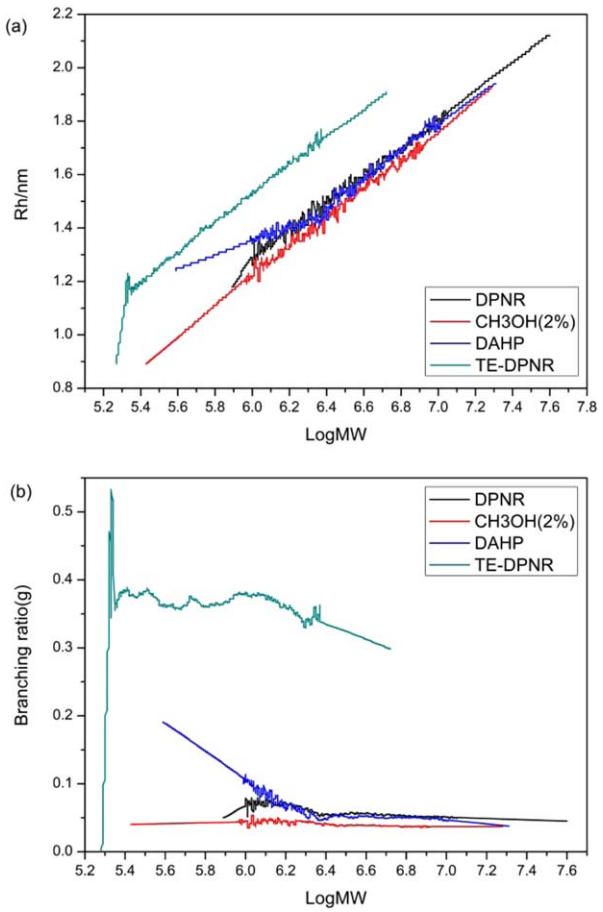

Figure 11. Distributions of (a) hydrodynamic radius, Rh, and (b) branching ratio, *g*, for the samples of DPNR, AE-DPNR treated with 2% CH_3OH, DPNR treated with DAHP, and TE-DPNR as a function of molar mass using linear standard PI as reference. [Color figure can be viewed in the online issue, which is available at wileyonlinelibrary.com.]

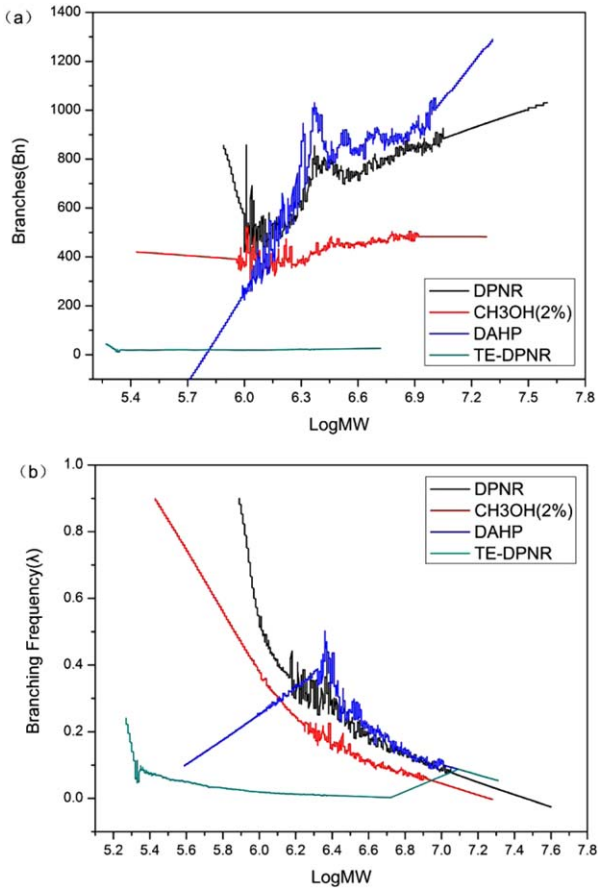

Figure 13. Distributions of (a) branches and (b) branching frequency for DPNR, AE-DPNR treated with 2% CH_3OH, DPNR treated with DAHP, and TE-DPNR as a function of molar mass using linear standard PI as reference. [Color figure can be viewed in the online issue, which is available at wileyonlinelibrary.com.]

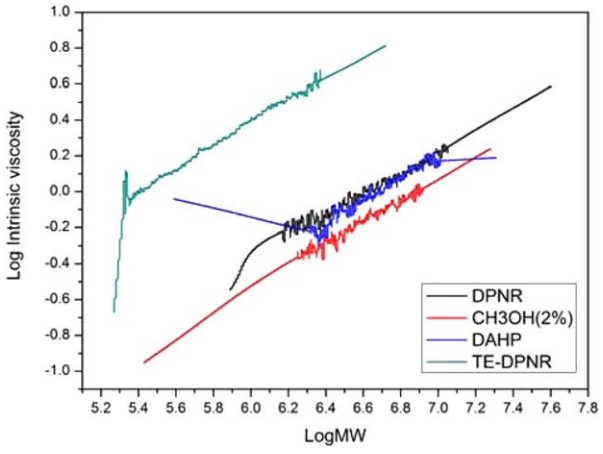

Figure 12. Mark–Houwink plots of the samples of DPNR, AE-DPNR treated with 2% CH_3OH, DPNR treated with DAHP, and TE-DPNR as a function of molar mass using linear standard PI as reference.The lines represent the fits of eq. (5). [Color figure can be viewed in the online issue, which is available at wileyonlinelibrary.com.]

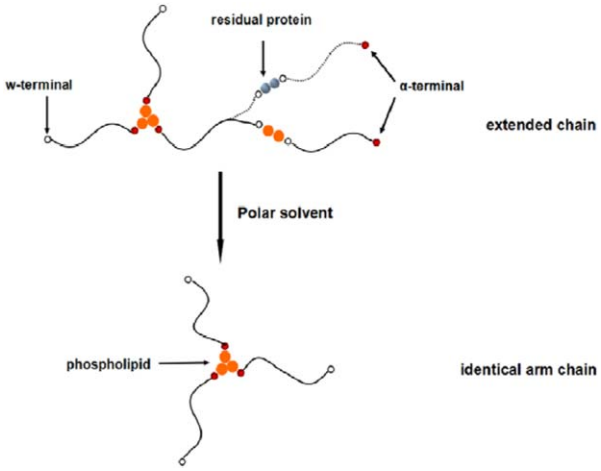

Figure 14. Extended chains with proposed structure and presumed structural change after the treatment with solvent in DPNR. [Color figure can be viewed in the online issue, which is available at wileyonlinelibrary.com.]

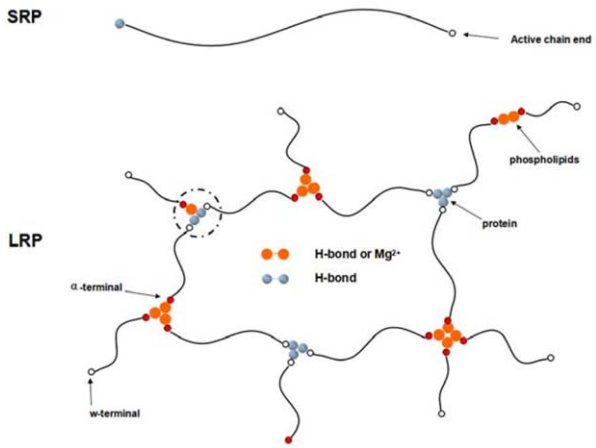

Figure 15. Assumed network structure in NR. [Color figure can be viewed in the online issue, which is available at wileyonlinelibrary.com.]

variation in the process of the treatment with polar solvent, as illustrated in Figure 14. During the variation from extended chains to identical arm chains, the degree of branching remains the same, but the viscosity goes down in the process. Here, the term "extended chains" refers to the chains that have bifunctional branch points instead of tri- or tetrafunctional branch points. There are two hypothetical structures of extended chains shown in Figure 14, including the ω-terminals connected with residual proteins or phospholipids. The assumption of residual proteins is based on the previous study that both residual proteins and fatty acids play a role in the formation of gel fractions, including the changes in physical properties in the deproteinized NR.[33] Nevertheless, the other assumption is more likely to happen, with the supporting evidence that the MWD of NR has not changed much after deproteinization, compared to the apparent bimodal MWD of TE-DPNR after transesterification. This assumption is also supported by the fact that the storage process of DPNR latex in the presence of ammonia shows an increase in gel content, which indicates that the functional groups at the ω-terminal can form branch points by interacting with phospholipids at the α-terminal or through micelle formation in DPNR.[8,34,35] Also, this variation is in good agreement with the phenomenon that the Bn of 2% CH_3OH–treated AE-DPNR does not increase as the molar mass increases, contrary to other samples. The longer DPNR rubber chain with the higher density of branch points is supposed to be decomposed worse than the shorter one after the treatment of polar solvent, leading to basically the same proportion of the bifunctional branch points in the rubber chain at a different MW fraction. As a consequence, the Bn of 2% CH_3OH–treated DPNR has little to do with molecular weight.

There might be another reason for the unconformity above that the removal of hydrogen bonding between branch points increases the free volume, which could effectively reduce the viscosity of the rubber solution along with a simultaneous decrease of Bn in the system. In terms of these results, the branch points in DPNR should originate mainly from the aggregation of phospholipids via hydrogen bonding because of the drastic decrease of Bn after the treatment with 2% CH_3OH. The considerable branching remaining in AE-DPNR with only a little decrease after the treatment with DAHP also give some evidence that some branch points in NR are constructed by ionic linkages like Mg^{2+}, though they have less effect.

According to the respective architectures of SRP and LRP along with the structure of the branched points, we can finally put forward a complete network of NR, as shown in Figure 15. SRPs are mostly linear macromolecules without any branched structure, and the protein bound on them may not participate in the branching formation because of the protein species, while the protein of LRPs, due to its amyloid properties, could quickly form large aggregates by hydrogen bonding. Except for the confirmatory formation mechanism of branch points, the interaction between protein and phospholipids may also play a role in the network of NR.[34]

CONCLUSIONS

By employing the GPC-DP-MALLS technique, the origin of the bimodal MWD and the branching architectures of NR are successfully revealed. The branching characterization of fractionated DPNR in conjunction with the changes in the MWD after transesterification constitutes powerful evidence for elucidating the coexistence of LRPs and SRPs with their respective structures. SRPs are mostly composed of linear molecules with no or few branches, while LRPs are expected to contain branch points originated from phospholipids to form branched molecules. The decreases in MW, gel content, and Bn after treatment with polar solvents suggest that the branch points are mainly formed by the association of phospholipids via hydrogen bonding. Ionic linkages, like Mg^{2+} ions, are regarded to rarely participate in the branching formation as well.

ACKNOWLEDGMENTS

This work was supported by National Natural Science Foundation of China (grant no. 51333003).

REFERENCES

1. Hwee, E. A.; Tanaka, Y. *Trends Polym. Sci.* **1993**, *3*, 493.
2. Tangpakdee, J.; Tanaka, Y. *Rubber Chem. Technol.* **1997**, *70*, 707.
3. Tarachiwin, L.; Sakdapipanich, J.; Ute, K.; Kitayama, T.; Tanaka, Y. *Biomacromolecules* **2005**, *6*, 1858.
4. Subramaniam, A. *Rubber Chem Technol.* **1972**, *45*, 346.
5. Fuller, K. N. G.; Fulton, W. S. *Polymer* **1990**, *31*, 4.
6. Tangpakdee, J.; Tanaka, Y. J. *Rubber Res.* **1997**, *12*, 112.
7. Mekkriengkrai, D.; Sakdapipanich, J. T.; Yasuyuki, T. *Rubber Chem Technol.* **2006**, *79*, 366.
8. Amnuaypornsri, S.; Tarachiwin, L.; Sakdapipanich, J. T. *J. Appl. Polym. Sci.* **2010**, *115*, 6.
9. Hubner, W.; Blume, A. *Chem. Phys. Lipids* **1998**, *96*, 99.
10. Tarachiwin, L.; Sakdapipanich, J. T.; Tanaka, Y. *Rubber Chem. Technol.* **2003**, *76*, 1177.

11. Tarachiwin, L.; Sakdapipanich, J. T.; Tanaka, Y. *Rubber Chem. Technol.* **2003**, *76*, 1185.
12. Archer, B. L.; Audley, B. G.; Cockbain, E. G.; McSweeney, G. P. *Biochem. J.* **1963**, *89*, 565.
13. Archer, B. L.; Cockbain, E. G. *Methods Enzymol.* **1969**, *15*, 476.
14. Tangpakdee, J.; Tanaka, Y.; Wititsuwannakul, R.; Chareonthiphakorn, N. *Phytochem.* **1996**, *42*, 2.
15. Tanaka, Y. *Rubber Chem. Technol.* **2001**, *74*, 355.
16. Sakdapipanich, J. T.; Suksujaritporn, S.; Tanaka, Y. J. *Rubber Res.* **1999**, *2*, 160.
17. Ohya, N.; Tanaka, Y.; Koyama, T. J. *Rubber Res.* **2000**, *3*, 214.
18. Oh, S. K.; Kang, H.; Shin, D. H. J. *Bio. Chem.* **1999**, *274*, 17132.
19. Tarachiwin, L.; Sakdapipanich, J. T.; Tanaka, Y. *Rubber Chem. Technol.* **2005**, *78*, 694.
20. Rojruthai, P.; Sakdapipanich, J. T.; Takahashi, S. J. *Biosci. Bioeng.* **2010**, *109*, 107.
21. Bristow, G. M.; George, M.; Westall, B. *Polymer* **1967**, *8*, 609.
22. Sakdapipanich, J. T. *J. Biosci. Bioeng.* **2007**, *103*, 287.
23. Sakdapipanich, J. T.; Kowitteerawut, T.; Suchiva, K. *Rubber Chem. Technol.* **1999**, *72*, 712.
24. Angulo-Sanchez, J. L.; Caballero-Mata, P. *Rubber Chem. Technol.* **1981**, *54*, 34.
25. Kim, C.; Sainte Beuve, J.; Guilbert, S. *Eur. Polym. J.* **2009**, *45*, 2249.
26. Makan, A. C.; Otte, T.; Pasch, H. *Macromolecules* **2012**, *45*, 5247.
27. Scholte, T. G. Characterization of long-chain Branching in polymers. Springer: Netherlands, **1983**; pp 1–37.
28. Grubisic, Z.; Rempp, P.; Benoit, H. *J. Polym. Sci. Polym. Lett.* **1967**, *5*, 753.
29. Zimm, B. H.; Stockmayer, W. H. *J. Chem. Phys.* **1949**, *17*, 1301.
30. Sansatsadeekul, J.; Sakdapipanich, J.; Rojruthai, P. *J. Biosci. Bioeng.* **2011**, *6*, 111.
31. Nawamawat, K.; Sakdapipanich, J. T.; Ho, C. C. *Colloids Surf., A* **2011**, *390*, 157.
32. Sakdapipanich, J. *Adv. Mater. Res.* **2014**, *844*, 498.
33. Nawamawat, K. Sakdapipanich J T, Ho C C. Macromolecular Symposia, **2010**, 288, 95.
34. Yunyongwattanakorn, J.; Tanaka, Y.; Kawahara, S. *Rubber Chem. Technol.* **2003**, *76*, 1228.
35. Tanaka, Y.; Tarachiwin, L. *Rubber Chem. Technol.* **2009**, *82*, 283.